Global-Scale Proxy System Modeling of Oxygen Isotopes in Lacustrine Carbonates: new insights from isotope-enabled-model proxy-data comparison

Matthew D. Jones[1*] and Sylvia G. Dee[2]

1. School of Geography, University of Nottingham, University Park, Nottingham. NG7 2RD matthew.jones@nottingham.ac.uk
2. Rice University, Department of Earth, Environmental, and Planetary Sciences, Houston, TX, USA. sylvia.dee@rice.edu

* corresponding author

Abstract

Proxy System Modelling (PSM) is now recognised as a crucial step in comparing climate model output with proxy records of past environmental change. PSMs filter the climate signal from the model, or from meteorological data, based on the physical, chemical and biological processes of the archive and proxy system under investigation. Here we use a PSM of lake carbonate $\delta^{18}O$ to forward model pseudoproxy time-series for every terrestrial grid square in the SPEEDY-IER isotope enabled General Circulation Model (GCM), and compare the results with 31 records of lake $\delta^{18}O$ data from the Americas in the NOAA Paleoclimate Database. The model-data comparison shows general patterns of spatial variability in the lake $\delta^{18}O$ data are replicated by the combination of SPEEDY-IER and the PSM, with differences largely explained by known biases in the models. The results suggest improved spatial resolution/coverage of climate models and proxy data, respectively, is required for improved data-model comparison, as are increased numbers of higher temporal resolution proxy time series (sub decadal or better) and longer GCM runs. We prove the concept of data-model comparison using isotope enabled GCMs and lake isotope PSMs and outline potential avenues for further work.

Keywords

Climate Variability; Lake Sedimentary Archives; Oxygen Isotopes; Proxy System Models; Isotope-Enabled GCMs

Highlights

- This paper presents the first global-scale forward modelling of lake carbonate $\delta^{18}O$.
- The proxy system model accounts for lake water and isotope balance, and converts lake water isotope values to a predicted carbonate $\delta^{18}O$ value.
- Forward modelled lake carbonate $\delta^{18}O$ is compared to a suite of available proxy data for the Americas, indicating moderate agreement between climate model and proxy data in terms of spatial trends.
- Data-model comparison proves the concept and approach used, with differences largely explained by known model biases.
- The new PSM provides avenues for future work comparing large proxy databases with isotope-enabled climate model simulations, as well as in paleoclimate data assimilation efforts.

1. Introduction

Changes in water availability, driven in part by changing hydroclimate, have been shown to have impacts on societies past (e.g. Cullen et al., 2000) and present (e.g. Kelley et al., 2015), and will inevitably impact the future (IPCC, 2014). Understanding the spatial and temporal patterns of hydroclimatic change and their forcings is therefore of paramount importance for planning for potential future changes in water resources (IPCC, 2014). To this end, the last two thousand years, and last millennium in particular (PAGES Hydro2k Consortium, 2017), provide invaluable data for investigating hydroclimate variability at scales useful for human populations at frequencies difficult to establish using the instrumental record. The spatial and temporal resolution of both paleoclimate proxy records, e.g. annual PDSI reconstructions from tree rings (Cook et al., 2016), and climate models (e.g. Jungclaus et al., 2017) run using the same configurations as those for historic and future projections, through the last two millennia (PAGES Hydro2k Consortium, 2017) also allows for improved proxy-data climate-model comparison (data-model comparison hereafter). This comparison is important for quantitatively constraining future climate projections, by expanding the test bed for climate models beyond the instrumental period, but also for iteratively improving our proxy data interpretations and climate model skill.

One such proxy is the ratio of stable isotopes of oxygen, a useful tracer of the hydrological cycle that preserves in multiple geological archives, the analysis of which is now commonplace. The long term monitoring programme of the Global Network for Isotopes in Precipitation (IAEA/WMO, 2018) and its analysis (Dansgaard, 1964; Bowen and Wilkinson, 2002), and studies at finer spatial scales (e.g. Good et al., 2014; Tyler et al., 2016) allow isotopic patterns in precipitation to be recognised and understood in the present day, and the range of archives that preserve a function of these patterns in the past potentially allows a long and spatially broad record of changes in hydroclimate through time to be reconstructed.

Lakes can provide long and continuous terrestrial records of past oxygen isotope change (usually reported using the delta notation, $\delta^{18}O$) and have a relatively good global coverage (e.g. Viau and Gajewski, 2001). $\delta^{18}O$ can be measured from a range of hosts within the sediment archive including cellulose, diatoms, and a range of carbonate hosts such as ostrocods, gastropods and sedimentary carbonate ($\delta^{18}O_{carb}$). Cellulose is generally considered to be a direct proxy of lake water isotope values ($\delta^{18}O_l$; e.g. Wolfe et al., 2007) whereas $\delta^{18}O_{carb}$ and $\delta^{18}O_{diatom}$ are functions of lake water temperature as well as $\delta^{18}O_l$ (e.g. Dean et al., 2018). At a first order lakes can provide i) a direct measurement of $\delta^{18}O_P$ or ii) the balance between precipitation amount and evaporation through time, depending on the hydrological setting of the lake (e.g. Leng and Marshall, 2004; Leng et al., 2006). However, there are multiple potential controls on $\delta^{18}O_l$ (e.g. Jones et al., 2005) and the actual controls will be specific for any given lake at a particular time. Process studies monitoring the isotopic systematics of a given lake (e.g. Jones et al., 2016; Cui et al., 2018) can aid understanding and thereby interpretation of downcore isotope records from an individual site (e.g. Steinman et al., 2010). Furthermore, the use of isotope mass balance models (such as the one employed in this study) can lead to quantification of these interpretations.

Lake isotope mass balance models are an example of a Proxy System Model (PSM), a forward process-driven model of all or part of the climate-archive-proxy system (e.g. Evans et al., 2013). The PSM mathematically approximates biological, geochemical, and physical changes that the proxy system itself imparts on the measured proxy signal. PSMs for multiple proxy types have been published in recent years, particularly for high-resolution (e.g. tree ring width) and water-isotope based systems (ice cores, corals, tree cellulose and speleothems) (Tolwinski-Ward et al., 2011, Evans et al., 2013; Dee et al., 2015a). These models have demonstrated their usefulness and flexibility, facilitating studies which enhance interpretation of climate signals recorded by proxy data (e.g. Anchukaitis et al., 2006; Baker et al., 2012; Steinman et al., 2013), diagnosing the specific impacts of proxy system processes on the final measurement (Dee et al., 2015a), improving data-model comparison by placing models and paleoclimate observations in the same reference frame or in the same units (e.g.Thompson et al., 2011, Dee et al., 2017), providing a critical and more physically-based step in paleoclimate data assimilation (Steiger et al., 2014, Dee et al., 2016), and in tracking uncertainties inherent to different proxy types (Dee et al., 2015a). PSMs provide an improved and quantifiable understanding of how proxies filter the input climate signal and subsequently encode it in a paleoclimate measurement.

Building upon previous work, we present here a forward model of intermediate complexity for $\delta^{18}O_l$ and $\delta^{18}O_{carb}$; the model is applicable globally, and adaptable to individual sites if needed. The forward model program and example input are publicly available (https://github.com/sylvia-dee/PRYSM) and coded in R (R Core Team, 2016), an open-source and free computational platform. Given that lake isotope PSMs have been shown to do a good job of predicting monitored lake water isotope values for individual sites (e.g. Jones et al., 2016) this paper aims to investigate the effectiveness of more generic PSMs, and their potential in allowing lake $\delta^{18}O$ records to be used as a data-model comparison tool. We first review previous work developing PSMs for isotopes in lacustrine archives (Section 2) and describe the model formulation and implementation for this study (Section 3). We demonstrate the efficiency and applications of this forward model, including data-model comparisons, using case studies of $\delta^{18}O_{carb}$ in section 4. Section 5 concludes by reviewing the model's performance and discuses caveats and avenues for future work.

2. Proxy System Modeling for Stable Water Isotopes in Lakes: a review

Paleoclimatic proxies in lake sediments experience multivariate climatic controls (e.g. Jones et al., 2005) including, depending on proxy type, temperature, precipitation, evaporation, humidity, wind speed, and atmospheric circulation changes. The multivariate nature of the climatic forcings on lake sedimentary archives necessitates the use of PSMs which incorporate both the input climate and the processes that govern the proxy's recording of that climate signal. PSMs can explicitly connect climate variable inputs (modeled or observed) to the proxy measurement while accounting for the non-climatic influences on that measurement. In doing so, such transfer models help partition between the climate signal of interest and noise imparted by hydrological and/or geological processes. These PSMs, as forward models, can convert climate model simulations to pseudoproxy records (the mathematical proxy record produced by the PSM) and are now considered a fundamental step for robust data-model comparison (PAGES Hydro2k Consortium, 2017).

Our PSM design follows previous work (Evans et al., 2013; Dee et al., 2015a) dividing the model into two different sub-components of the proxy system response to climate forcing, both of which serve a unique purpose: first, an *Environment Model* accounts for the impacts of the regional or local climatic impacts at the proxy measurement site; for lakes in particular, this includes the local hydrology of the lake system. Second, the *Sensor Model* describes the physical, geochemical and/or biological response of the proxy measured to environmental forcing.

2.1 Environment Model: Hydrology & Lake Water Balance

Isotope mass balance models have been used extensively to investigate lake hydrology (e.g. Dincer, 1968; Gat, 1995; Gibson et al., 2002) and quantitatively infer past climate change (Benson and Paillet, 2002; Jones et al., 2007; Steinman et al., 2010; Steinman et al., 2013). The models are based on variations of the following mass balance approach, where for a given, well-mixed, lake:

$$dV/dt = P + Qi - E - Qo \quad (1)$$

where V is the lake volume, t, time, P, precipitation on lake surface per unit time, E is evaporation from lake surface per unit time and Q_0 and Q_i are the sums of other outlflows and inflows respectively, usually a combination of groundwater and surfacewater, measured in the same units as P and E.

The isotopic components of the lake must also similarly vary, for example in a lake where surface and groundwater inflows are meteoric water:

$$\frac{d}{dt}(V\delta_l) = P\delta_P + Qi\delta_P - E\delta_E - Qo\delta_l \quad (2)$$

where δ_P, δ_E and δ_l are the isotope values of the precipitation, evaporation and lake waters respectively.

δ_E is difficult to measure and is therefore usually calculated (e.g. Steinman et al., 2010) using equations based on the evaporation model of Craig and Gordon (1965), for example:

$$\delta_E = (\alpha^* \delta_l - h\delta_A - \varepsilon)/(1 - h + (0.001\varepsilon_k)) \quad (3)$$

where α* is the equilibrium isotopic fractionation factor dependent on the temperature at the evaporating surface e.g. as defined by Majoube (1971). *h* is the relative humidity normalised to the saturation vapour pressure at the temperature of the air water interface (e.g. Steinman et al., 2010) and ε_k is the kinetic fractionation factor e.g. as defined by Gonfiantini (1986). δ_A is the isotopic value of the air vapour over the lake and $\varepsilon = \varepsilon^* + \varepsilon_k$ where $\varepsilon^* = 1000(1-\alpha^*)$.

2.2 Sensor Model: Isotope Proxy Measurements from Lake Sediments

$\delta^{18}O$ as a proxy can be measured from a range of hosts, so-called *sensors* within the PSM sub-model framework (Evans et al., 2013), within lake sediments (see introduction). Here we focus on lake carbonates. $\delta^{18}O_{carb}$ is a function of $\delta^{18}O_l$ and temperature, with the degree of temperature fractionation depending on the type of calcium carbonate precipitated in the lake waters. For calcite the fractionation between mineral and water (α) is expressed (Kim and O'Neil, 1997) as

$$1000 \ln \alpha_{(calcite\text{-}water)} = 18.03(10^3 T^{-1}) - 32.42 \qquad (4)$$

where T is temperature (K), whereas for aragonite (Kim et al., 2007)

$$1000 \ln \alpha_{(aragonite\text{-}water)} = 17.88(10^3 T^{-1}) - 31.14 \qquad (5)$$

Given seasonal variability in $\delta^{18}O_l$ and temperature the timing of carbonate precipitation is therefore important. The timing of carbonate precipitation is a function of the concentration of bicarbonate and calcium ions in the lake waters, lake water temperature and pH (Kelts and Hsu, 1978), which can be controlled by biological activity as well as physical changes in the lake system e.g. (Shapley et al., 2005). Isotopic measurements from biogenic carbonates can have additional species-specific vital effects, related to local $\delta^{18}O_l$ values within lake sub-habitats, or additional fractionation effects during shell growth (e.g. van Hardenbroek et al., 2018).

For our work here we do not run modeled $\delta^{18}O_{carb}$ through a model of sediment deposition that would take into account variability in the amount of carbonate precipitated in a given year, or sampling or chronological issues. PSM sub-models which account for chronological uncertainties and post-depositional effects such as bioturbation are forthcoming in companion and recently published work (e.g. Dee et al., in revision; Doman & Laepple, 2018).

3. Methods

Here, we present an adapted version of the forward model developed in Jones and Imbers (2010) and Jones et al. (2016) to model changes in $\delta^{18}O_l$ and $\delta^{18}O_{carb}$, specifically from authigenic calcite. We drive a simplified version of this lake isotope forward model with output from the isotope-enabled atmospheric GCM, SPEEDY-IER (Dee et al., 2015b) using R. The R script used to generate the pseudoproxy data discussed here is given in the Supplementary Information and is available from https://github.com/sylvia-dee/PRYSM.

The analysis presented in this work requires a GCM simulation of sufficient length to assess decadal- to centennial-scale variability, sufficient resolution to provide sub-annual timesteps, as well as embedded water stable isotope physics. While other higher resolution isotope-enabled GCMs may offer a more advanced representation of atmospheric dynamics, most of these models are computationally expensive, and have not yet performed publicly available last-millennium simulations with water isotopes. SPEEDY-IER is an intermediate complexity atmospheric GCM (at resolution T31 or 3.75 x 3.75 degrees), and is a relatively efficient option for long paleoclimate integrations. Despite some simplifications to the model's physics, SPEEDY-IER simulates climatic and water isotope fields that are comparable with higher-order AGCMs at a much lower computational cost. For this study, SPEEDY-IER was forced with sea surface temperatures from the last millennium simulation (Landrum et al., 2013) of the CCSM4 coupled model (Gent et al., 2011), spanning 850-2005 AD; we extracted monthly data from model years 1000-2005 AD for this study.

For the PSM's *Environment* sub-model, we assume a relatively straightforward lake hydrology, where the isotopic values of all water entering the lake (i.e. precipitation, groundwater and surface waters) is meteoric, and a minimum amount of inflow or outflow is required to maintain a lake in the basin given changes in evaporation and precipitation. Model lakes have a simple morphology such that lake area does not change with lake volume.

As a first-principles experiment, we forward model $\delta^{18}O_l$ records at monthly time steps for a theoretical lake in every terrestrial grid cell in the climate model for the duration of the model run. We model a lake at each end of the hydrological gradient i.e. a fully open and fully closed lake, thereby modelling the potential range of $\delta^{18}O_{carb}$, acknowledging that most lakes will lie somewhere between these two extremes.

3.1 Forward Model Inputs: Hydrology

The hydrology, i.e. non isotopic components, of modelled lakes must also balance. For open lakes, with negligible evaporative control, we keep volumes constant for each monthly time step, with lake outflows equivalent to monthly inputs, taken here as twice the monthly precipitation value, to account for on lake and catchment inputs (see R code in Supplementary Information).

For closed lakes, in addition to the precipitation and evaporation components available directly from the climate model a ground-/surface-water component is also required. For a given lake, this component (Q) must be equal to P-E over the study period for the lakes to remain in near steady state (i.e. so the lake doesn't disappear or become unrealistically deep), such that for lakes in grid squares where P>E, Q will be positive and represent outflow, and where E>P, Q is negative and represents some inflow to the system. The value of P-E for a given grid square is therefore an important first-order control on the modeled lake hydrological balance. Here we calculate Q, indicating inflow vs. outflow, (see R code in the Supplementary Information) as a monthly constant based on the mean precipitation and evaporation values, from SPEEDY-IER, through the study period (Fig. 1a). Prior to use in the model any negative values of evaporation from SPEEDY-IER are replaced by values of 0.5 mm/day; values of 0 do not work for the forward model equations.

Lake volumes can then be calculated, from an initial starting point, for each monthly time step of the model. Initial lake volumes are based on a relatively small lake, with an area of 12,500 m^2 and a depth of 8m. To ensure a lake continues to exist in each grid square throughout the study period, initial volumes (Vo) for each grid square are recalculated if required after an initial run such that volumes for all grid squares are always above zero throughout the last millennium (Fig. 1b).

A useful byproduct of any lake isotope mass balance model, which requires a correct estimate of changing volume, is therefore a direct simulation of lake volume change through time, which can provide a useful metric for further data-model comparison for an individual lake system (e.g. Jones et al., 2016), or in the context of syntheses of lake level change (e.g. Street-Perrot et al., 1989, Hostetler & Bartlein, 1990).

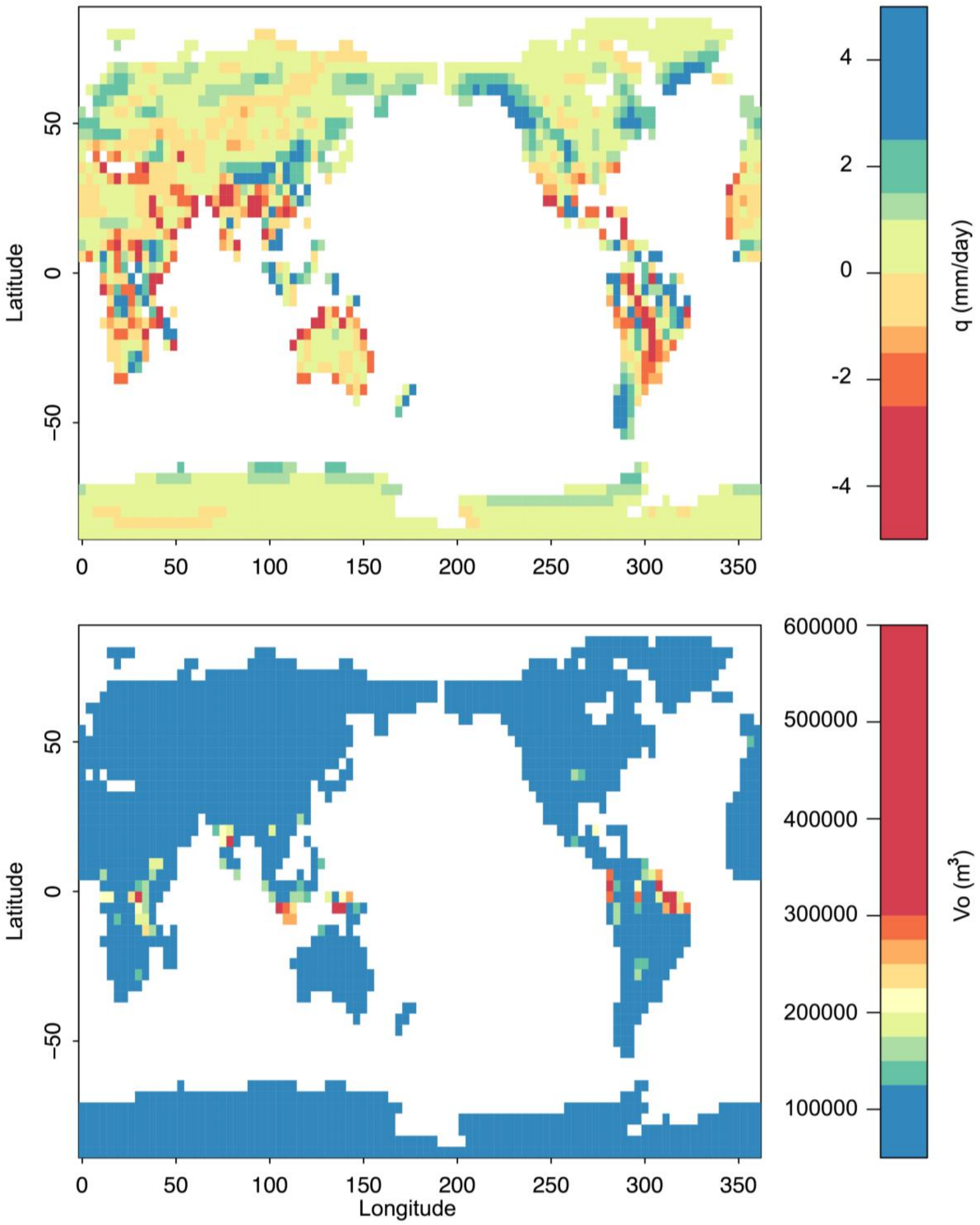

Figure 1 Mean annual values of q (p-e) and initial lake volumes (Vo) for all terrestrial SPEEDY-IER grid squares.

3.2 Forward Model Inputs: Isotopes

Intial values of δ_I are based on the mean values of δ_P from the full model time window. SPEEDY-IER's simulation of precipitation isotopes closer to the poles is limited by errors in the ability of the spectral dynamical core to advect very low humidity values; this leads to water isotope ratios in vapor and precipitation that are positively biased compared to observations. As a result, modelled $\delta^{18}O_P$ at the poles are too positive in SPEEDY-IER compared to to GNIP data (Dee et al., 2015b), by up to 10-15‰ at the highest latitudes. We correct for this here by using the relationship between bias and temperature poleward of 30° described in Dee et al (2015b).

For the additional components needed for the closed lake systems, δ_A is taken directly from SPEEDY-IER. It is recognised (e.g. Gibson et al., 2016; Lacey and Jones, this issue) that large lakes will impact their own hydrology, including changing values of δ_A to include components of the evaporating lake waters. This is unlikely to impact the small basins modelled here, but would impact model-data comparison for larger lake sites if not accounted for. Lake inflow in months with no precipitation are given mean δ_P values for that grid square.

Relative humidity and temperature values were extracted directly from SPEEDY-IER. Given known terrestrial temperature biases on the order of +1-3°K in SPEEDY-IER (Dee et al., 2015b) we use a temperature bias correction of -2°K for all grid squares. Lake temperatures also often differ from air temperatures above the lake (e.g. Sharma et al., 2008), and the difference between these temperatures is an important control on *h*. Based on 341 measurement of summer lake temperatures, measured by satellite or *in situ*, compared to air temperatures from the National Centres for Environmental Prediction (NCEP) and the Climatic Research Unit (CRU) in a global database (Sharma et al., 2015) lake temperatures are, on average, 1.5 degrees warmer than air temperatures (mean values of +1.4 for comparisons with NCEP data and +1.6 when compared to CRU). Although there is variability around this mean value, including lakes with cooler water temperatures than air temperatures, there are no clear spatial (latitude, longitude, altitude) or morphological (lake volume, surface area or maximum depth) controls on the difference between lake and air temperatures in the database such that we take the average of +1.5 degrees for all lakes modelled here. Values of *h* are then calculated following Steinman et al. (2010); see R code for details.

Values of the equilibrium (α^*) and kinetic (ε_k) fractionation factors are calculated from the corrected temperature and *h* values following the equations of Majoube (1971) and Gonfiantini (1986) respectively. With high relative humidity values the resulting values of ε_k change sign, impacting calculations of δ_E, such that *h* values were capped at 98%. Values of δ_l for each time step for each grid square can then be calculated following the model equations from Jones et al. (2016); see R code in the Supplementary Information.

3.3 Sensor Model

Values for $\delta^{18}O_{carb}$ were then calculated based on the calcite temperature fractionation equation (equation 4) of Kim and O'Neil (1997) using the rearrangement of this equation from Leng and Marshall (2004). Classical authigenic lake carbonates typically precipitate in summer months (e.g. Dean et al., 2015) following late spring algal blooms and/or ion concentration due to evaporation and here we calculate an annual value of $\delta^{18}O_{carb}$ for the lake in each SPEEDY-IER grid square based on δ_l and temperature values for January and June for southern and northern hemisphere lakes respectively.

4. Results and Discussion: Data-Model Comparison for Lake Carbonate Systems

Straightforward comparisons between climate model output and proxy observation is confounded by a number of uncertainties, outlined, for example, in Ault et al. (2013). First, the impacts of the proxy system itself on the measured signal, potentially unrelated to climate, must be accounted for. We address this directly with the construction of the lake carbonate PSM presented in this work, but acknowldege the realtively low level of complexity in the PSM used. The PSMs used here restrict the hydrological complexity of the model lakes; the degree of hydrological closue of a given lake can impact its isotopic sensitivity to climate change for example (Jones and Imbers, 2010). In general, however, these potential PSM biases are site specific, and are therefore not possible to generalise for a model applied at the global scale. We would take a different approach, using a more complex PSM if the aim of our study was to compare an individual site, or a small group of sites, to climate model output, rather than the global-scale view employed here.

Second, climate models contain biases, and simulate internal variability which is inherently different from that recorded by paleoclimate data (e.g. Dee et al., 2017). We have discussed known biases in SPEEDY-IER, and how these have been accounted for in this study in the previous section, and discuss variability later in the paper. In addition, as with other GCMs, SPEEDY-IER's grid cells of 3.75 degrees, equating to approximately 176,400 square kilometers, dwarf the often-microclimate scale of the lakes. Due to these limitations, of both PSMs and GCMs, we thereofore do not expect that point-based comparisons can necessarily yield meaningful information about model-data agreement nor fully inform model-data discrepancies, however global scale trends should still be evident.

We have circumvented these challenges where possible by translating the climate model output to proxy units using the PSM, and comparing time-scale dependent variances and broad spatial trends in both the model and data, rather than looking for direct site-grid square comparisons. The data used are extracted from the NOAA Paleoclimate Database (https://www.ncdc.noaa.gov/data-access/paleoclimatology-data). We extracted relevant data by searching with the query *Paleolimnology > oxygen isotopes* between the years 1000 to -50 cal years BP. This resulted in 53 available data sets. 41 of these are from the Americas, with only 3 from Europe and Africa, so we focus here on the Americas for data model comparisons to maximize our ability to use as large a range of data sites as possible, whilst having some constraint on space given global isotopic and climatic gradients. Of these 41 datasets, we removed records from non-carbonate hosts, such as diatoms, resulting in a final dataset of 31 lake sites with $\delta^{18}O_{carb}$ data records to compare with the pseudoproxy data sets (Table 1).

4.1 Spatial variability

Figure 2 shows the mean annual $\delta^{18}O_{carb}$ simulated by the open and closed lake PSMs in each terrestrial GCM grid cell. In agreement with theory, the forward-modeled lakes indicate more evaporative enrichment of $\delta^{18}O_{carb}$ in the subtropics (e.g. Australia, the Southwestern U.S.) and more depleted $\delta^{18}O_{carb}$ values in the tropics (e.g. Amazon & Congo basins) and toward the poles. The open lake PSM results which reflect the weighted average of δ_P, show the general trend towards more negative isotopic values of precipitation at the poles and more continental areas

(Bowen and Wilkinson, 2002). The greater divergence between open and closed lakes at mid latitudes (c. 30° N and S) would be expected given evaporation is more often a control of lake isotope records, resulting in more positive values of δ_l and $\delta^{18}O_{carb}$, at these latitudes (e.g. Roberts et al., 2008).

To evaluate and compare spatial variability in the model and the data directly, Figure 3 compares lake isotope data from the Americas with the latitudinal patterns evident in the forward model results. If the SPEEDY-IER model variable output and the PSM's subsequent simulation of $\delta^{18}O_{carb}$ agree with observations, most lake carbonate data through the last millennium should fall between the blue and green lines in Fig. 3, representing open and closed lakes. This comparison shows that the general spatial trends of lake $\delta^{18}O_{carb}$ data, particularly the latitudinal gradient, are well simulated by the PSM and SPEEDY-IER.

To look at the data-model differences in more detail we compared proxy data and pseudoproxy time-series from the 12 sites amongst our 31-site data list that have temporal resolution approaching that of SPEEDY-IER i.e. more than one data point per 10 years (Fig. 4). For the open lakes Lime Lake data shows similar values to the open lake PSM, as does Martin Lake for some parts of the record (Fig. 4). The large range of $\delta^{18}O_{carb}$ values from the Martin Lake core are driven by changes in the dominant rainfall source area through the record (Bird et al., 2017). The PSM-data comparison suggest here that SPEEDY-IER does a good job of reconstructing $\delta^{18}O_p$ values similar to present day, but does not reconstruct the dramatic changes in rainfall source area related to the Pacific North American pattern recorded by the Martin Lake sediments. Data-PSM comparison of Steel Lake also suggests a good match, with the $\delta^{18}O_{carb}$ values closely matching the open lake PSM pseudoproxy values (Fig. 4). However, Tian et al. (2006) interpret the core data from Steel Lake as being influenced by evaporation, due to some isotopic measurements of modern lake waters and calibration of recent sediment $\delta^{18}O_{carb}$ with P-AET measurements. The lake is described as having a small stream running through it and having some groundwater influence, such that evaporation may be less influential than described, however it also possible that the $\delta^{18}O_p$ bias correction applied here to SPEEDY-IER at higher latitudes is not sufficient at Steel Lake (46°58'N), such that the pseudoproxy data for both open and closed lakes are too positive.

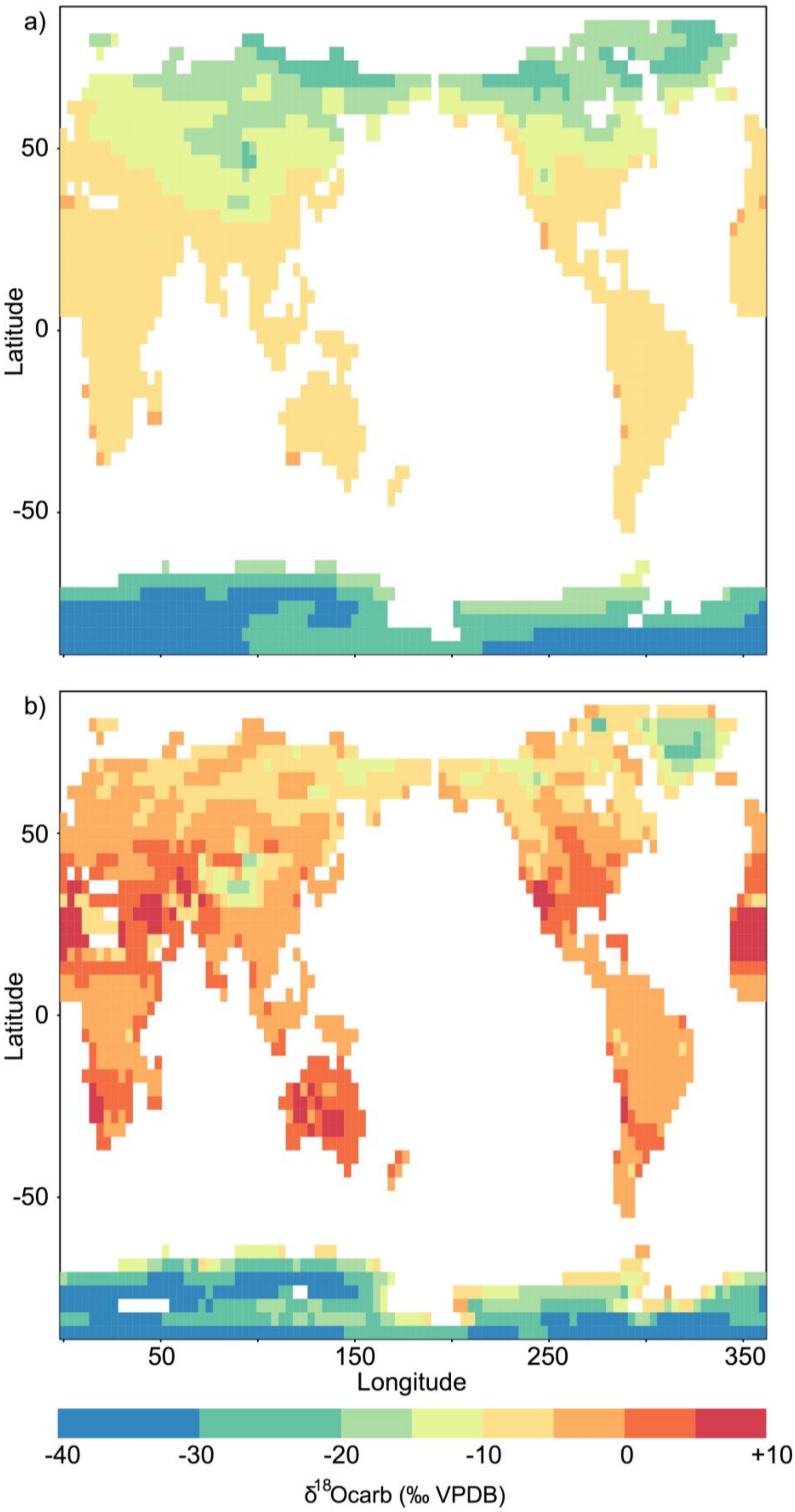

Figure 2 Mean annual carbonate values simulated from a) open and b) closed lake forward models in each SPEEDY-IER grid square for the last millennium.

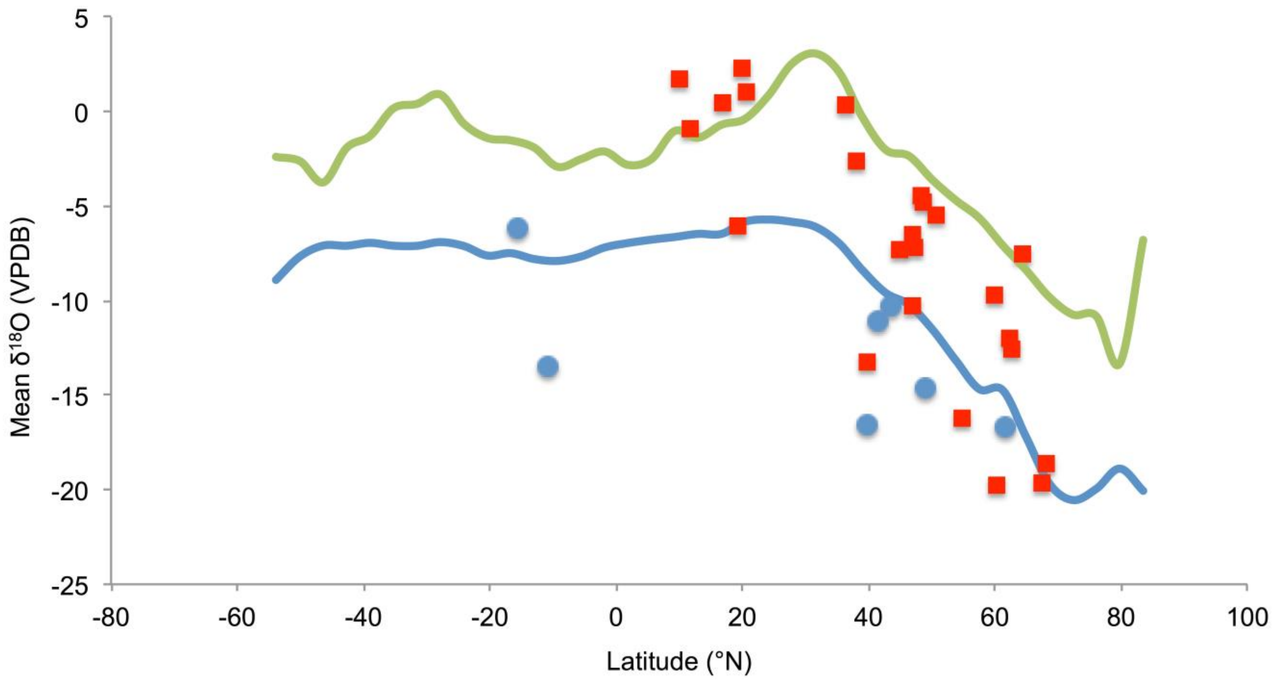

Figure 3 Comparison of latitudinal patterns in $\delta^{18}O_{carb}$ in the Americas from forward modelled open (blue) and closed (green) lakes compared to data from the NOAA Paleoclimate Database (Table 1) from both open (blue circles) and closed (red squares) lakes.

Three other open lake sites do have $\delta^{18}O_{carb}$ data more negative than the open lake PSM pseudoproxy data. Pumacocha and Bison Lake are extremely high elevation sites compared to the others shown in Figure 4 (4300 and 3255 m.a.s.l. respectively). Topography in SPEEDY is not well resolved so there are known biases in capturing the full amount effect (Dee et al., 2015b) that could not be systematically corrected for here. Kepler Lake is the highest latitude site (61.6°N) of the twelve shown in Fig. 4. It is possible that the negative data offset compared to the open lake PSM here is therefore due to an underestimation of the latitudinal bias correction used, as suggested for Steel Lake. There are also potential hydrological reasons that could cause this offset, with high latitude and high altitude sites potentially more impacted isotopically by snow melt, which would likely lead to a negative isotope bias compared to a direct precipitation input to the lake (e.g. Beria et al., 2018).

Cleland, Castor, Foy and Mono Lakes sit, as would be expected, within the theoretical end member PSM lakes for their locations. The two remaining sites Aguada X'caamal and El Gancho have data that are more positive than the closed lake pseudoproxy records (Fig. 4). This suggests that inputs to the system are isotopically too negative in the PSM. SPEEDY-IER tends to have a positive bias in $\delta^{18}O_p$, although more so at high latitudes, and there is relatively little GNIP data through Latin America with which to compare models or data to. Another possibility is that water at these sites is evaporated before entering the groundwater, e.g. in the soil, causing evaporative enrichment that is not adequately represented in the PSM framework.

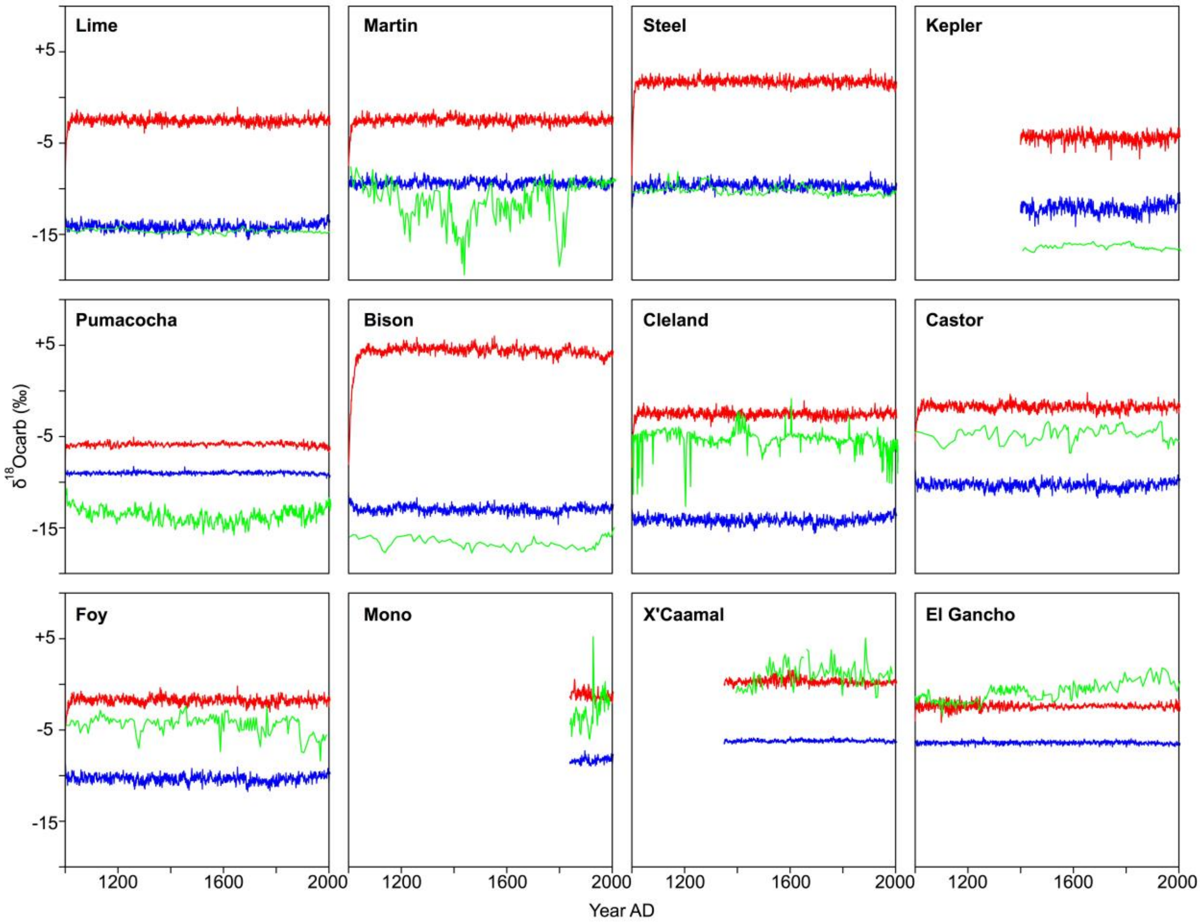

Figure 4 Comparison of pseudoproxy time series from open (blue) and closed (red) lake PSMs from the equivalent SPEEDY-IER grid squares of the 12 high resolution lake $\delta^{18}O_{carb}$ data sets (Table 1).

In summary, looking at the variance of lake isotope records in *space*, this work confirms that first order lake PSMs coupled to an intermediate-complexity climate model can resolve observed continental patterns in $\delta^{18}O_{carb}$ data, whilst further informing our interpretation of some of these records, and helping to diagnose the impacts of biases in the climate model and PSM.

4.2 Temporal patterns and variability

Recent work has highlighted the fact that even with the additional information provided by a proxy system model, observations from paleoclimate archives show larger temporal variability at decadal to centennial timescales than GCMs, and PSMs driven with their output, currently simulate (Laepple & Huybers, 2014, Dee et al., 2017). This is evident in the records shown in Figure 4 where the $\delta^{18}O_{carb}$ data, even at lower resolution than the pseudoproxy records, tend to show greater variability, with the exception of some of the open lake records such as Kepler and Lime.

Greater variability in closed lakes, compared to open systems, is what would be expected from lake isotope theory (e.g. Leng and Marshall, 2004; Roberts et al., 2008) and previous modelling studies (Jones and Imbers, 2010). This is also evident in the PSM output here e.g. when comparing variability in open and closed lake $\delta^{18}O_{carb}$ pseudoproxy records across the Americas (Fig. 5).

Comparing the power spectral densities (PSDs) between proxy and pseudoproxy data provides a way of comparing the dominant modes of variability in both time-series. We compare the 12 highly resolved data records and their pseudoproxy equivalent time-series in this way (Figure 6) using the open or closed PSM output where appropriate. Using this approach Dee et al. (2017) found that PSMs of a number of proxies, including speleothem and coral carbonates $\delta^{18}O$, whilst helping to resolve model-data differences at interannual to decadal timescales, could not account for a mismatch in variance at multi-decadal to centennial timescales. Our results here tell a similar story.

In nearly all cases the proxy data show more power at lower frequencies compared to the pseudoproxy time series, with the pseudoproxy time series having more power at higher, sub-decadal, frequencies (Fig. 6). Exceptions to this are for Pumacocha, where the PSD curves are very similar for both data and pseudoproxy time series, and to some degree for Bison Lake. It is interesting to note that these two open sites, at high elevation, which have data more negative data than the equivalent PSMs both show the closest match in term of temporal variability between the data and PSM output.

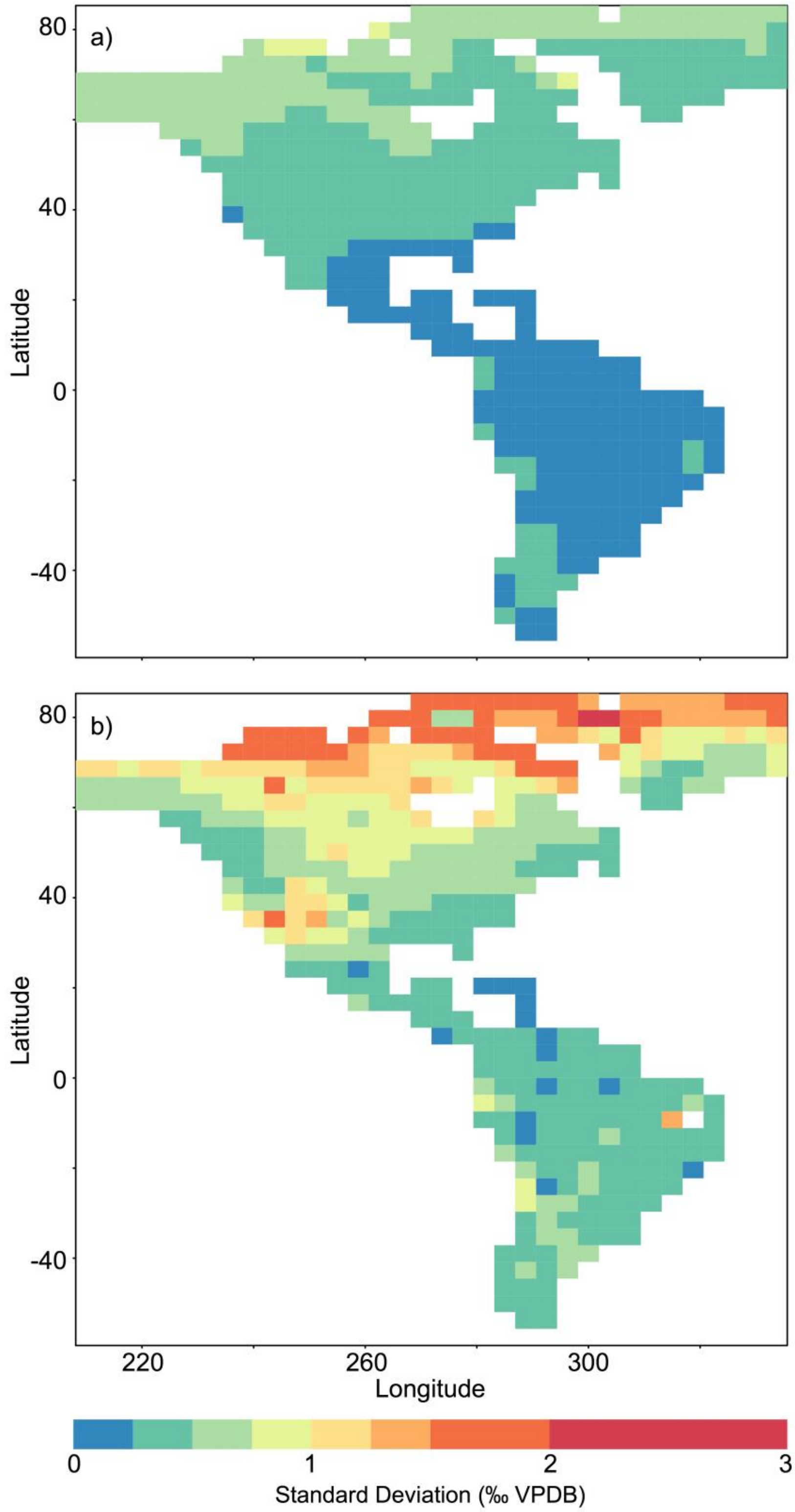

Figure 5 Standard deviation of psudoproxy $\delta^{18}O_{carb}$ time series from a) open and b) closed lakes in each grid square in the Americas through the last millennium.

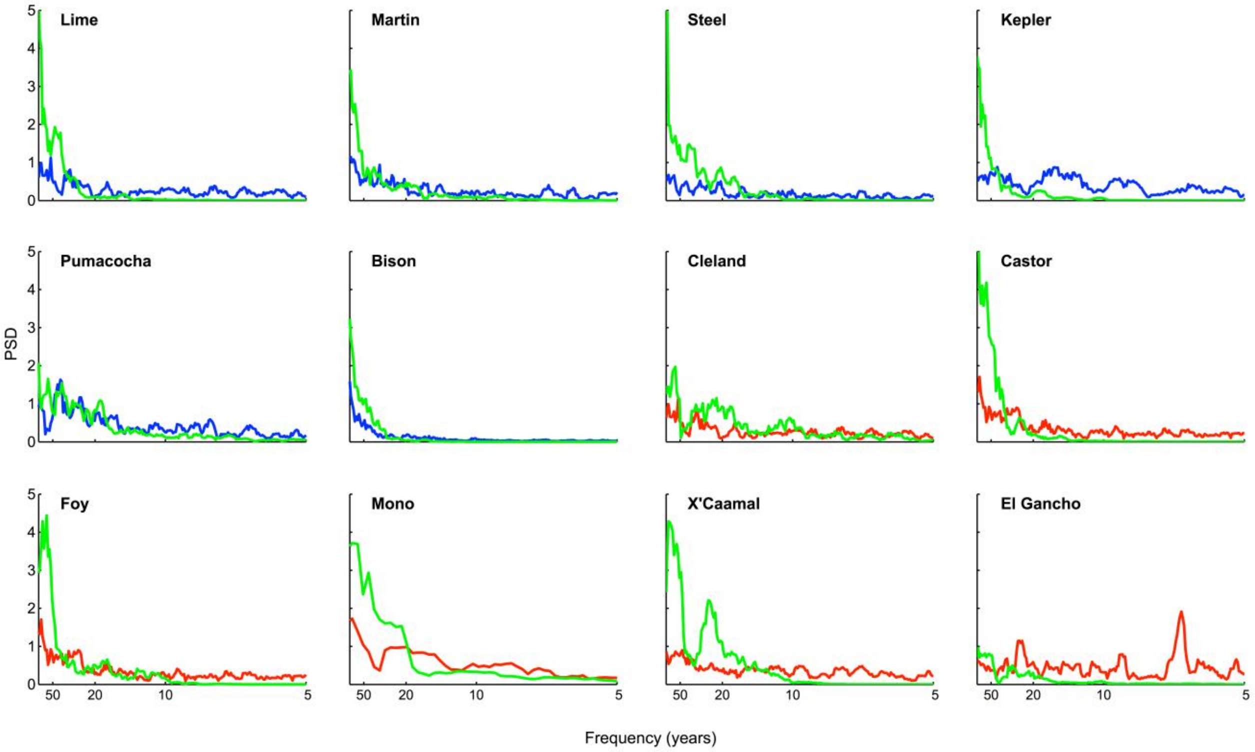

Figure 6 Comparison of the power spectra from data and pseudoproxy time-series from open (blue) and closed (red) lake PSMs. We estimate power spectra of the PSM pseudoproxy data and the proxy data, interpolated to annual resolution, using Thomson's multi-taper method (Thomson, 1982).

Given their length and continuity lake records provide a potentially important check on lower frequency climate modes simulated by GCMs. The comparisons here suggests that resolving lower frequency variability observed in proxy data, with the exception here of some higher elevation locations, remains a challenge for GCMs, even when filtered by a PSM. Further work on PSM complexity may also help further understand this issue.

5. Summary

The work presented here further develops our understanding of forward modeling paleoclimate archives; moving towards best practices in data-model comparison by creating physically-based transfer functions to translate between the variables of climate model output and the multivariate (and sometimes nonlinear) signals encoded in paleoclimate data (Evans et al., 2013, Dee et al, 2015a).

Recent efforts to compile large, standardized databases of paleoclimate data spanning the last 2 millennia, beyond those employed in this work, and including, but not limited to Pages2k (PAGES 2k Consortium, 2017) and Iso2k (Konecky et al., 2017) are providing an invaluable new platform for the investigation of temporal, and spatial trends characterizing Earth's climate through the last two millennia. Alongside paleoclimate model intercomparison projects, such as PMIP3 (Brannocot et al., 2011, 2012) and the forthcoming PMIP4 (Kageyama et al., 2016), they provide opportunities for large-scale data-model comparison to constrain hydroclimate variability in space and time. These comparisons will require PSMs for multiple proxy types and the approach introduced in this paper will help facilitate this further.

The approach in this paper may also facilitate broader use of lake data in paleoclimate data assimilation and paleoclimate reanalysis products (e.g. Steiger et al., 2014, Hakim et al., 2016, Dee et al., 2016). To date, these studies have only employed annually-resolved proxy data, however the framework for assimilating data unevenly spaced in time is operational (Malevitch et al., 2017). Thus, work such as that presented here provides a new link for the assimilation of lake sedimentary records in paleoclimate reanalyses.

We were limited here to just one isotope-enabled model simulation. SPEEDY-IER is an intermediate-complexity AGCM, and thus houses temperature and precipitation bias which influence the PSM's pseudoproxy output. Indeed, a PSM's output is inherently limited by the climate model or observational data used to drive the model. However, future work will examine whether higher-order isotope-enabled GCMs might improve comparisons with observations. Additional millennial-scale simulations which include water isotopes are becoming increasingly available, and we will repeat these experiments with higher-order GCM simulations and more complex lake PSMs to check the impacts of intermediate-complexity biases explicitly in future work. As more proxy data become available this will further increase the usefuleness of such data-model comparisons, and work such as that presented here presents challenges to both data and model communities to improve the products available for data-model comparison, for example

GCMs that better simuate higher lattitude $\delta^{18}O_p$ or improving the spatial spread of proxy data available for comparison.

Lake sedimentary archives constitute one of the richest data sources for hydroclimatic reconstructions given their broad global coverage and temporal lengthscales. Characterizing climate variability on multi-decadal to centennial timescales from these archives is crucial for validating the 'slow-physics,' or low-frequency variability component in climate models, outside the relatively brief purview of 20th century observations. To this end, we hope that this work provides a step forward for extracting the most meaningful signals from lacustrine carbonates, with full appreciation for stable water isotope physics operating in the atmosphere, as well as lake hydrology. Data-model comparison techniques which account for confounding proxy system impacts will only strengthen our interpretations of these data, enhancing our understanding of processes occurring on the landscape and informing our interpretations of atmospheric variability as captured by the proxy data. Taken together, this information provides more robust constraints for climate model simulations of long-term variability, essential for useful future climate projections.

Acknowledgemnts

We thank Stephen Phipps, Sam Stevenson, and James Russell for helpful discussions at various stages of this work. Thanks to Adam Algar and George Swann for R coding encouragement and support. We thank two anonymous reviewers for their helpful comments on a previous version of the manuscript. This work was supported in part by the Peter Voss Postdoctoral Fellowship granted to S. Dee at Brown University, and the University of Texas Institute for Geophysics Postdoctoral Fellowship.

References

Anchukaitis, K.J., Evans, M.N., Kaplan, A., Vaganov, E.A., Hughes, M.K., Grissino-Mayer, H.D., Cane, M.A., 2006. Forward modeling of regional scale tree-ring patterns in the southeastern United States and the recent influence of summer drought. Geophysical Research Letters 33, n/a-n/a.

Anderson, L., 2011. Holocene record of precipitation seasonality from lake calcite δ18O in the central Rocky Mountains, United States. Geology 39, 211-214.

Anderson, L., 2012. Rocky Mountain hydroclimate: Holocene variability and the role of insolation, ENSO, and the North American Monsoon. Glob. Planet. Change 92-93, 198-208.

Anderson, L., Abbott, M.B., Finney, B.P., Burns, S.J., 2005. Regional atmospheric circulation change in the North Pacific during the Holocene inferred from lacustrine carbonate oxygen isotopes, Yukon Territory, Canada. Quat. Res. 64, 21-35.

Anderson, L., Abbott, M.B., Finney, B.P., Burns, S.J., 2007. Late Holocene moisture balance variability in the southwest Yukon Territory, Canada. Quat. Sci. Rev. 26, 130-141.

Anderson, L., Finney, B.P., Shapley, M.D., 2011. Lake carbonate-δ18O records from the Yukon Territory, Canada: Little Ice Age moisture variability and patterns. Quat. Sci. Rev. 30, 887-898.

Anderson, R.Y., Dean, W.E., Bradbury, J.P., 1993. Elk Lake in perspective. SPECIAL PAPERS-GEOLOGICAL SOCIETY OF AMERICA, 1-1.

Ault, T.R., Cole, J.E., Overpeck, J.T., Pederson, G.T., George, S.S., Otto-Bliesner, B., Woodhouse, C.A., Deser, C., 2013. The Continuum of Hydroclimate Variability in Western North America during the Last Millennium. J. Clim. 26, 5863-5878.

Baker, A., Bradley, C., Phipps, S., Fischer, M., Fairchild, I., Fuller, L., Spötl, C., Azcurra, C., 2012. Millennial-length forward models and pseudoproxies of stalagmite [delta] 18O: an example from NW Scotland. Climate of the Past 8, 1153.

Beria, H., Larsen, J.R., Ceperley, N.C., Michelon, A., Vennemann, T., Schaefli, B., 2018 Understanding snow hydrological processes through the lens of stable water isotopes. Wiley Interdisciplinary Reviews: Water 0, e1311.

Benson, L., Paillet, F., 2002. HIBAL: a hydrologic-isotopic-balance model for application to paleolake systems. Quat. Sci. Rev. 21, 1521-1539.

Bhattacharya, T., Byrne, R., Böhnel, H., Wogau, K., Kienel, U., Ingram, B.L., Zimmerman, S., 2015. Cultural implications of late Holocene climate change in the Cuenca Oriental, Mexico. Proceedings of the National Academy of Sciences 112, 1693-1698.

Bird, B.W., Abbott, M.B., Vuille, M., Rodbell, D.T., Stansell, N.D., Rosenmeier, M.F., 2011. A 2,300-year-long annually resolved record of the South American summer monsoon from the Peruvian Andes. Proceedings of the National Academy of Sciences 108, 8583-8588.

Bird, B.W., Wilson, J.J., Gilhooly Iii, W.P., Steinman, B.A., Stamps, L., 2017. Midcontinental Native American population dynamics and late Holocene hydroclimate extremes. Scientific Reports 7, 41628.

Bowen, G., Wilkinson, B., 2002. Spatial distribution of δ18O in meteoric precipitation. Geology 30, 315-318.

Braconnot et al, Evaluation of climate models using palaeoclimatic data, Nature Climate Change 2, 417-424 (2012), doi:10.1038/nclimate1456

Braconnot et al, The Paleoclimate Modeling Intercomparison Project contribution to CMIP5, CLIVAR Exchanges No. 56, Vol. 16, No.2, May 2011, pp 15-19

Chipman, M.L., Clegg, B.F., Hu, F.S., 2012. Variation in the moisture regime of northeastern interior Alaska and possible linkages to the Aleutian Low: inferences from a late-Holocene δ18O record. J. Paleolimn. 48, 69-81.

Clegg, B.F., Hu, F.S., 2010. An oxygen-isotope record of Holocene climate change in the south-central Brooks Range, Alaska. Quat. Sci. Rev. 29, 928-939.

Cook, B.I., Anchukaitis, K.J., Touchan, R., Meko, D.M., Cook, E.R., 2016. Spatiotemporal drought variability in the Mediterranean over the last 900 years. Journal of Geophysical Research: Atmospheres.

Craig, H., Gordon, L.I., 1965. Deuterium and oxygen 18 variations in the ocean and the marine atmosphere.

Cullen, H.M., deMenocal, P.B., Hemming, S., Hemming, G., Brown, F.H., Guilderson, T., Sirocko, F., 2000. Climate change and the collapse of the Akkadian empire: Evidence from the deep sea. Geology 28, 379-382.

Curtis, J.H., Brenner, M., Hodell, D.A., 1999. Climate change in the Lake Valencia Basin, Venezuela, ~12600 yr BP to present. The Holocene 9, 609-619.

Curtis, J.H., Brenner, M., Hodell, D.A., Balser, R.A., Islebe, G.A., Hooghiemstra, H., 1998. A multi-proxy study of Holocene environmental change in the Maya Lowlands of Peten, Guatemala. J. Paleolimn. 19, 139-159.

Cui, J., Tian, L., Gibson, J.J., 2018. When to conduct an isotopic survey for lake water balance evaluation in highly seasonal climates. Hydrol. Process. 32, 379-387.

Dansgaard, W., 1964. Stable isotopes in precipitation. Tellus 16, 436-468.

Dean, J.R., Eastwood, W.J., Roberts, N., Jones, M.D., Yiğitbaşıoğlu, H., Allcock, S.L., Woodbridge, J., Metcalfe, S.E., Leng, M.J., 2015. Tracking the hydro-climatic signal from lake to sediment: A field study from central Turkey. Journal of Hydrology 529, Part 2, 608-621.

Dean, J.R., Jones, M.D., Leng, M.J., Metcalfe, S.E., Sloane, H.J., Eastwood, W.J., Roberts, C.N., 2018. Seasonality of Holocene hydroclimate in the Eastern Mediterranean reconstructed using the oxygen isotope composition of carbonates and diatoms from Lake Nar, central Turkey. The Holocene 28, 267-276.

Dee, S., Emile-Geay, J., Evans, M.N., Allam, A., Steig, E.J., Thompson, D.M., 2015(a). PRYSM: An open-source framework for PRoxY System Modeling, with applications to oxygen-isotope systems. Journal of Advances in Modeling Earth Systems 7, 1220-1247.

Dee, S., Noone, D., Buenning, N., Emile-Geay, J., Zhou, Y., 2015(b). SPEEDY-IER: A fast atmospheric GCM with water isotope physics. J. Geophys. Res.-Atmos. 120, 73-91.

Dee, S.G., Steiger, N.J., Emile-Geay, J., Hakim, G.J., 2016. On the utility of proxy system models for estimating climate states over the common era. Journal of Advances in Modeling Earth Systems 8, 1164-1179.

Dee, S.G., Parsons, L.A., Loope, G.R., Overpeck, J.T., Ault, T.R., Emile-Geay, J., 2017. Improved spectral comparisons of paleoclimate models and observations via proxy system modeling: Implications for multi-decadal variability. Earth Planet. Sci. Lett. 476, 34-46.

Dee, S.G., Russell, J. M., Morrill, C., Chen, Z., *in revision.* PRYSM v. 2.0: A Proxy System Model for Lacustrine Archives. Paleoceanography & Paleoclimatology.

Dinçer, T., 1968. The Use of Oxygen 18 and Deuterium Concentrations in the Water Balance of Lakes. Water Resources Research 4, 1289-1306.

Dolman, A. M., & Laepple, T. (2018). Sedproxy: a forward model for sediment archived climate proxies. *Climate of the Past Discussions*, 1-31.

Ekdahl, E.J., Fritz, S.C., Baker, P.A., Rigsby, C.A., Coley, K., 2008. Holocene multidecadal- to millennial-scale hydrologic variability on the South American Altiplano. The Holocene 18, 867-876.

Evans, M.N., Tolwinski-Ward, S.E., Thompson, D.M., Anchukaitis, K.J., 2013. Applications of proxy system modeling in high resolution paleoclimatology. Quat. Sci. Rev. 76, 16-28.

Gat, J.R., 1995. Stable isotopes of fresh and saline lakes, Physics and chemistry of lakes. Springer, pp. 139-165.

Gent, P.R., Danabasoglu, G., Donner, L.J., Holland, M.M., Hunke, E.C., Jayne, S.R., Lawrence, D.M., Neale, R.B., Rasch, P.J., Vertenstein, M., Worley, P.H., Yang, Z.L., Zhang, M.H., 2011. The Community Climate System Model Version 4. J. Clim. 24, 4973-4991.

Gibson, J.J., Prepas, E.E., McEachern, P., 2002. Quantitative comparison of lake throughflow, residency, and catchment runoff using stable isotopes: modelling and results from a regional survey of Boreal lakes. Journal of Hydrology 262, 128-144.

Gonfiantini, R., 1986. Environmental isotopes in lake studies. Handbook of Environmental Isotope Geochemistry; The Terrestrial Environment, 113-168.

Gonyo, A.W., Yu, Z., Bebout, G.E., 2012. Late Holocene change in climate and atmospheric circulation inferred from geochemical records at Kepler Lake, south-central Alaska. J. Paleolimn. 48, 55-67.

Good, S.P., Mallia, D.V., Lin, J.C., Bowen, G.J., 2014. Stable Isotope Analysis of Precipitation Samples Obtained via Crowdsourcing Reveals the Spatiotemporal Evolution of Superstorm Sandy. Plos One 9, e91117.

Grossman, E.L., Ku, T.L., 1986. Oxygen and Carbon Isotope Fractionation in Biogenic Aragonite - Temperature Effects. Chem. Geol. 59, 59-74.

Hakim, G.J., Emile-Geay, J., Steig, E.J., Noone, D., Anderson, D.M., Tardif, R., Steiger, N., Perkins, W.A., 2016. The last millennium climate reanalysis project: Framework and first results. Journal of Geophysical Research: Atmospheres 121, 6745-6764.

Hiner, C.A., Kirby, M.E., Bonuso, N., Patterson, W.P., Palermo, J., Silveira, E., 2016. Late Holocene hydroclimatic variability linked to Pacific forcing: evidence from Abbott Lake, coastal central California. J. Paleolimn. 56, 299-313.

Hodell, D.A., Brenner, M., Curtis, J.H., Guilderson, T., 2001. Solar Forcing of Drought Frequency in the Maya Lowlands. Science 292, 1367-1370.

Hodell, D.A., Brenner, M., Curtis, J.H., Medina-González, R., Ildefonso-Chan Can, E., Albornaz-Pat, A., Guilderson, T.P., 2005. Climate change on the Yucatan Peninsula during the Little Ice Age. Quat. Res. 63, 109-121.

Hostetler, S.W., Bartlein, P.J., 1990. Simulation of lake evaporation with application to modeling lake level variations of Harney-Malheur Lake, Oregon. Water Resources Research 26, 2603-2612.

Hu, F.S., Ito, E., Brown, T.A., Curry, B.B., Engstrom, D.R., 2001. Pronounced climatic variations in Alaska during the last two millennia. Proceedings of the National Academy of Sciences 98, 10552-10556.

IAEA, WMO, 2018. Global Network of Isotopes in Precipitation. The GNIP Database.

IPCC, 2014: Climate Change 2014: Synthesis Report. Contribution of Working Groups I, II and III to the Fifth Assessment Report of the Intergovernmental Panel on Climate Change [Core Writing Team, R.K. Pachauri and L.A. Meyer (eds.)]. IPCC, Geneva, Switzerland, 151 pp.

Jungclaus, J.H., Bard, E., Baroni, M., Braconnot, P., Cao, J., Chini, L.P., Egorova, T., Evans, M., González-Rouco, J.F., Goosse, H., Hurtt, G.C., Joos, F., Kaplan, J.O., Khodri, M., Klein Goldewijk, K., Krivova, N., LeGrande, A.N., Lorenz, S.J., Luterbacher, J., Man, W., Maycock, A.C., Meinshausen, M., Moberg, A., Muscheler, R., Nehrbass-Ahles, C., Otto-Bliesner, B.I., Phipps, S.J., Pongratz, J., Rozanov, E., Schmidt, G.A., Schmidt, H., Schmutz, W., Schurer, A., Shapiro, A.I., Sigl, M., Smerdon, J.E., Solanki, S.K., Timmreck, C., Toohey, M., Usoskin, I.G., Wagner, S., Wu, C.J., Yeo, K.L., Zanchettin, D., Zhang, Q., Zorita, E., 2017. The PMIP4 contribution to CMIP6 – Part 3: The last millennium, scientific objective, and experimental design for the PMIP4 past1000 simulations. Geosci. Model Dev. 10, 4005-4033.

Jones, M.D., Cuthbert, M.O., Leng, M.J., McGowan, S., Mariethoz, G., Arrowsmith, C., Sloane, H.J., Humphrey, K.K., Cross, I., 2016. Comparisons of observed and modelled lake δ18O variability. Quat. Sci. Rev. 131, 329-340.

Jones, M.D., Imbers, J., 2010. Modeling Mediterranean lake isotope variability. Glob. Planet. Change 71, 193-200.

Jones, M.D., Leng, M.J., Eastwood, W.J., Keen, D.H., Turney, C.S.M., 2002. Interpreting stable-isotope records from freshwater snail-shell carbonate: a Holocene case study from Lake Golhisar, Turkey. Holocene 12, 629-634.

Jones, M.D., Leng, M.J., Roberts, C.N., Turkes, M., Moyeed, R., 2005. A coupled calibration and modelling approach to the understanding of dry-land lake oxygen isotope records. J. Paleolimn. 34, 391-411.

Jones, M.D., Roberts, C.N., Leng, M.J., 2007. Quantifying climatic change through the last glacial-interglacial transition based on lake isotope palaeohydrology from central Turkey. Quat. Res. 67, 463-473.

Kageyama, M., Braconnot, P., Harrison, S.P., Haywood, A.M., Jungclaus, J., Otto-Bliesner, B.L., Peterschmitt, J.Y., Abe-Ouchi, A., Albani, S., Bartlein, P.J. and Brierley, C., 2016. PMIP4-CMIP6: the contribution of the Paleoclimate Modelling Intercomparison Project to CMIP6. *Geoscientific Model Development Discussions*.

Kelts, K., Hsü, K.J., 1978. Freshwater Carbonate Sedimentation, In: Lerman, A. (Ed.), Lakes: Chemistry, Geology, Physics. Springer New York, New York, NY, pp. 295-323.

Kim, S.T., ONeil, J.R., 1997. Equilibrium and nonequilibrium oxygen isotope effects in synthetic carbonates. Geochim. Cosmochim. Acta 61, 3461-3475.

Kim, S.-T., O'Neil, J.R., Hillaire-Marcel, C., Mucci, A., 2007. Oxygen isotope fractionation between synthetic aragonite and water: Influence of temperature and Mg2+ concentration. Geochim. Cosmochim. Acta 71, 4704-4715.

Konecky, B.L. et al., 2017 Global Synthesis of Common Era Hydroclimate using Water Isotope Proxies from Multiple Archives: First Results from the PAGES Iso2k Project Abstract PP43D-03 presented at 2017 Fall Meeting, AGU, New Orleans, LA, 11-15 Dec.

Lacey, J. and Jones, M.D. *in press* Quantitative reconstruction of early Holocene and last glacial climate on the Balkan Peninsula using coupled hydrological and isotope mass balance modelling. Quat. Sci. Rev

Laepple, T., Huybers, P., 2014. Ocean surface temperature variability: Large model–data differences at decadal and longer periods. Proceedings of the National Academy of Sciences 111, 16682-16687.

Landrum, L., Otto-Bliesner, B.L., Wahl, E.R., Conley, A., Lawrence, P.J., Rosenbloom, N., Teng, H.Y., 2013. Last Millennium Climate and Its Variability in CCSM4. J. Clim. 26, 1085-1111.

Leng, M.J., Marshall, J.D., 2004. Palaeoclimate interpretation of stable isotope data from lake sediment archives. Quat. Sci. Rev. 23, 811-831.

Leng, M.J., Lamb, A.L., Heaton, T.H.E., Marshall, J.D., Wolfe, B.B., Jones, M.D., Holmes, J.A., Arrowsmith, C., 2006. Isotopes in lake sediments, Isotopes in palaeoenvironmental research. Springer, pp. 147-184.

Li, H.-C., Ku, T.-L., Stott, L.D., Anderson, R.F., 1997. Stable isotope studies on Mono Lake (California). 1. d18 in lake sediments as proxy for climatic change during the last 150 years. Limnol. Oceanogr. 42, 230-238.

Majoube, M., 1971. Fractionnement en oxygène 18 et en deutérium entre l'eau et sa vapeur. J. Chim. Phys. 68, 1423-1436.

Malevitch, S.B., Tierney, J.E., Hakim, G.J. and Tardif, R. 2017 A fresh look at the Last Glacial Maximum using Paleoclimate Data Assimilation PP13C-1092 presented at 2017 Fall Meeting, AGU, New Orleans, LA, 11-15 Dec.

PAGES Hydro2k Consortium, 2017. Comparing proxy and model estimates of hydroclimate variability and change over the Common Era. Clim. Past 13, 1851-1900.

PAGES 2k Consortium, 2017. A global multiproxy database for temperature reconstructions of the Common Era. Scientific Data 4, 170088.

R Core Team Team, 2016. R: A Language and Environment for Statistical Computing.

Roberts, N., Jones, M.D., Benkaddour, A., Eastwood, W.J., Filippi, M.L., Frogley, M.R., Lamb, H.F., Leng, M.J., Reed, J.M., Stein, M., Stevens, L., Valero-Garces, B., Zanchetta, G., 2008. Stable isotope records of Late Quaternary climate and hydrology from Mediterranean lakes: the ISOMED synthesis. Quat. Sci. Rev. 27, 2426-2441.

Shapley, M.D., Ito, E., Donovan, J.J., 2005. Authigenic calcium carbonate flux in groundwater-controlled lakes: Implications for lacustrine paleoclimate records. Geochim. Cosmochim. Acta 69, 2517-2533.

Shapley, M.D., Ito, E., Donovan, J.J., 2009. Lateglacial and Holocene hydroclimate inferred from a groundwater flow-through lake, Northern Rocky Mountains, USA. The Holocene 19, 523-535.

Stansell, N.D., 2013. Lacustrine stable isotope record of precipitation changes in Nicaragua during the Little Ice Age and Medieval Climate Anomaly. Geology 41, 151-154.

Steiger, N.J., Hakim, G.J., Steig, E.J., Battisti, D.S., Roe, G.H., 2014. Assimilation of Time-Averaged Pseudoproxies for Climate Reconstruction. J. Clim. 27, 426-441.

Steinman, B.A., Abbott, M.B., Mann, M.E., Stansell, N.D., Finney, B.P., 2012. 1,500 year quantitative reconstruction of winter precipitation in the Pacific Northwest. Proceedings of the National Academy of Sciences 109, 11619-11623.

Steinman, B.A., Abbott, M.B., Nelson, D.B., Stansell, N.D., Finney, B.P., Bain, D.J., Rosenmeier, M.F., 2013. Isotopic and hydrologic responses of small, closed lakes to climate variability: Comparison of measured and modeled lake level and sediment core oxygen isotope records. Geochim. Cosmochim. Acta 105, 455-471.

Steinman, B.A., Pompeani, D.P., Abbott, M.B., Ortiz, J.D., Stansell, N.D., Finkenbinder, M.S., Mihindukulasooriya, L.N., Hillman, A.L., 2016. Oxygen isotope records of Holocene climate variability in the Pacific Northwest. Quat. Sci. Rev. 142, 40-60.

Steinman, B.A., Rosenmeier, M.F., Abbott, M.B., 2010. The isotopic and hydrologic response of small, closed-basin lakes to climate forcing from predictive models: Simulations of stochastic and mean-state precipitation variations. Limnol. Oceanogr. 55, 2246-2261.

Stevens, L.R., Stone, J.R., Campbell, J., Fritz, S.C., 2006. A 2200-yr record of hydrologic variability from Foy Lake, Montana, USA, inferred from diatom and geochemical data. Quat. Res. 65, 264-274.

Street-Perrott, F., Marchand, D., Roberts, N., Harrison, S., 1989. Global lake-level variations from 18,000 to 0 years ago: A palaeoclimate analysis. Oxford University (UK).

Thompson, D.M., Ault, T.R., Evans, M.N., Cole, J.E., Emile-Geay, J., 2011. Comparison of observed and simulated tropical climate trends using a forward model of coral δ18O. Geophysical Research Letters 38, n/a-n/a.

Thomson, D.J., 1982. Spectrum estimation and harmonic analysis. Proc. IEEE 70 (9), 1055–1096.

Tian, J., Nelson, D.M., Hu, F.S., 2006. Possible linkages of late-Holocene drought in the North American midcontinent to Pacific Decadal Oscillation and solar activity. Geophysical Research Letters 33, n/a-n/a.

Tolwinski-Ward, S.E., Evans, M.N., Hughes, M.K., Anchukaitis, K.J., 2011. An efficient forward model of the climate controls on interannual variation in tree-ring width. Climate Dynamics 36, 2419-2439.

Tyler, J.J., Jones, M., Arrowsmith, C., Allott, T., Leng, M.J., 2016. Spatial patterns in the oxygen isotope composition of daily rainfall in the British Isles. Climate Dynamics 47, 1971-1987.

van Hardenbroek, M., Chakraborty, A., Davies, K.L., Harding, P., Heiri, O., Henderson, A.C.G., Holmes, J.A., Lasher, G.E., Leng, M.J., Panizzo, V.N., Roberts, L., Schilder, J., Trueman, C.N., Wooller, M.J., 2018. The stable isotope composition of organic and inorganic fossils in lake sediment records: Current understanding, challenges, and future directions. Quat. Sci. Rev. 196, 154-176.

Viau, A.E., Gajewski, K., 2001. Holocene variations in the global hydrological cycle quantified by objective gridding of lake level databases. Journal of Geophysical Research: Atmospheres 106, 31703-31716.

Whitlock, C., Dean, W.E., Fritz, S.C., Stevens, L.R., Stone, J.R., Power, M.J., Rosenbaum, J.R., Pierce, K.L., Bracht-Flyr, B.B., 2012. Holocene seasonal variability inferred from multiple proxy records from Crevice Lake, Yellowstone National Park, USA. Palaeogeography, Palaeoclimatology, Palaeoecology 331-332, 90-103.

Wolfe, B.B., Falcone, M.D., Clogg-Wright, K.P., Mongeon, C.L., Yi, Y., Brock, B.E., Amour, N.A.S., Mark, W.A., Edwards, T.W.D., 2007. Progress in isotope paleohydrology using lake sediment cellulose. J. Paleolimn. 37, 221-231.

Wooller, M.J., Kurek, J., Gaglioti, B.V., Cwynar, L.C., Bigelow, N., Reuther, J.D., Gelvin-Reymiller, C., Smol, J.P., 2012. An ~11,200 year paleolimnological perspective for emerging archaeological findings at Quartz Lake, Alaska. J. Paleolimn. 48, 83-99.

Yu, Z., Eicher, U., 1998. Abrupt Climate Oscillations During the Last Deglaciation in Central North America. Science 282, 2235-2238.

Table 1 Lake carbonate records from the last millennium in the NOAA paleoclimate database used in this study. *High resolution sites (see text for discussion).

Site Name	Latitude	Longitude	Mean $\delta^{18}O_{carb}$ (‰)	σ $\delta^{18}O_{carb}$ (‰)	Lake Hydrology (Open/Closed)	Reference
Keche	68.02	-146.92	-18.57	0.71	Closed	Chipman et al., 2012
Takahula	67.35	-153.66	-19.70	1.73	Closed	Clegg and Hu, 2010
Quartz	64.20	-149.82	-7.50	0.91	Closed	Wooller et al., 2012
Farewell	62.55	-153.63	-12.55	0.13	Closed	Hu et al., 2001
Seven Mile	62.17	136.38	-11.99	0.59	Closed	Anderson et al., 2011
*Kepler**	61.55	-149.20	-16.70	0.29	Open	Gonyo et al., 2012
Jellybean	60.35	-134.80	-19.76	0.33	Closed	Anderson et al., 2005
Marcella	60.07	-133.80	-9.71	1.02	Closed	Anderson et al., 2007
Paradise	54.69	-122.62	-16.26	0.40	Closed	Steinman et al., 2016
*Cleland**	50.83	-116.39	-5.44	1.19	Closed	Steinman et al., 2016
*Lime**	48.87	-117.34	-14.63	0.20	Open	Steinman et al., 2012
*Castor**	48.54	-119.56	-4.80	0.71	Closed	Steinman et al., 2012
*Foy**	48.17	-114.35	-4.49	1.02	Closed	Stevens et al., 2006
Elk	47.20	-95.25	-7.21	0.42	Closed	Anderson et al., 1993
Jones	47.05	-113.14	-6.49	0.71	Closed	Shapley et al., 2009
*Steel**	46.97	-94.68	-10.29	0.47	Closed	Tian et al., 2006
Crevice	45.00	-110.58	-7.30	0.95	Closed	Whitlock et al., 2012
Crawford	43.47	-79.95	-10.30	0.88	Open	Yu and Eicher,1998
*Martin**	41.56	-85.38	-11.10	2.23	Open	Bird et al., 2017
*Bison**	39.75	-107.33	-16.60	0.59	Open	Anderson, 2011
Yellow	39.65	-107.35	-13.28	0.44	Closed	Anderson, 2012
*Mono**	38.00	-119.00	-2.64	1.57	Closed	Li et al., 1997
Abbott	36.23	-121.48	0.32	1.61	Closed	Hiner et al., 2016
*X'caamal**	20.60	-88.28	1.06	1.28	Closed	Hodell et al., 2005
Chichancanab	19.88	-88.77	2.28	0.63	Closed	Hodell et al., 2001
Aljojuca	19.09	-97.53	-6.02	2.67	Closed	Bhattacharya et al., 2015
Peten Itza	16.92	-89.83	0.51	0.24	Closed	Curtis et al., 1998
*El Gancho**	11.90	-85.92	-0.93	0.94	Closed	Stansell et al., 2013
Valencia	10.17	-67.75	1.75	0.54	Closed	Curtis et al., 1999
*Pumacocha**	-10.70	-76.06	-13.44	0.68	Open	Bird et al., 2011
Umayo	-15.44	-70.10	-6.12	0.98	Open	Ekdahl et al., 2008